

Sediment detachment by rain power

Emmanuel J. Gabet

Department of Geological Sciences, University of California, Santa Barbara, California, USA

Thomas Dunne

Donald Bren School of Environmental Science and Management and Department of Geological Sciences, University of California, Santa Barbara, Santa Barbara, California, USA

Received 6 June 2001; revised 23 May 2002; accepted 23 May 2002; published 3 January 2003.

[1] In interrill areas, overland flow is often incapable of detaching soil particles so detachment is primarily by raindrop impact. We derive a mathematical expression, rain power (R , $W m^{-2}$), relating the energy expenditure of raindrops impacting a soil surface to the rate of detachment of soil particles. Rain power incorporates rainfall, hillslope, and vegetation characteristics and is modulated by flow depths. Rainfall simulation experiments on natural hillslopes were performed to measure detachment rates and across-slope flow depth distributions in surface runoff. Our results indicate that flow depths follow a Poisson distribution, and this observation is used to develop a dimensionless function, $A(\bar{h}, d)$, that accounts for the interaction of flow depths (h) and raindrop diameter (d) in moderating detachment rates. Rain power correlates well with the detachment rate of fine-grained particles (ψ , $g m^{-2} s^{-1}$) so that $\psi = 0.011R^{1.4}A(\bar{h}, d)$ ($n = 44$, $R^2 = 0.88$, $p < 0.005$). We generalize this result to represent natural rainfall conditions and present a method for modeling sediment detachment rates and sediment discharge along entire lengths of hillslopes under the range of conditions where detached sediment is transported as wash load. Modeling simulations demonstrate the temporal and spatial variation in detachment rates caused by increases in flow depth.

INDEX TERMS: 1815 Hydrology: Erosion and sedimentation; 1824 Hydrology: Geomorphology (1625); 1860 Hydrology: Runoff and streamflow; *KEYWORDS:* overland flow, rainsplash, sheetflow, grazing, washload, kinematic wave

Citation: Gabet, E. J., and T. Dunne, Sediment detachment by rain power, *Water Resour. Res.*, 39(1), 1002, doi:10.1029/2001WR000656, 2003.

1. Introduction

1.1. Previous Work

[2] It has long been recognized that raindrop impact detaches soil particles that may be subsequently transported by overland flow [e.g., Ellison, 1947]. The importance of raindrop impact in sediment detachment has been shown in both laboratory [e.g., Young and Wiersma, 1973] and field settings [e.g., Hudson, 1957] and an extensive body of literature has been published on the subject (see Salles *et al.* [2000] for a concise review). Indeed, the effect of raindrop impact has been incorporated into the most commonly used model for predicting soil erosion, the universal soil loss equation [Smith and Wischmeier, 1962], and its successor, the watershed erosion prediction project [Zhang *et al.*, 1998]. Most investigations into this process have relied on factor analysis and multiple regressions to predict sediment detachment based on various combinations of parameters. These parameters have included rainfall properties such as drop size and velocity [Salles *et al.*, 2000], drop circumference [Gilley and Finkner, 1985], drop momentum [Kneale, 1982], kinetic energy [Ekern, 1950; Wischmeier, 1959], and rainfall intensity [Meyer, 1981; Zhang *et al.*, 1998]. Other variables have included landscape character-

istics such as slope angle [McCool *et al.*, 1987] and vegetation cover [Nearing *et al.*, 1989]. In this study, we derive a mathematical expression, from a basic physical principle, that unites many of these parameters.

1.2. Rain Power

[3] When a drop of rain strikes a patch of soil, the kinetic energy of the drop is transferred to soil particles and to water on the surface, detaching soil particles and displacing water. We use the term, rain power, to describe the rate at which this energy is transferred to the surface. Rain power per unit area is the time derivative of the kinetic energy per unit area. To derive rain power, we begin with a mass of water per unit area impacting a bare soil surface:

$$\frac{\text{mass}}{\text{area}} = \rho i t \cos \theta, \quad (1)$$

where ρ is the density of water (1000 kg m^{-3}), i is rainfall intensity (m s^{-1}), t is storm duration (s), and θ is hillslope angle. The rainfall flux is corrected by the hillslope angle to represent the distribution of rainfall over the planar surface area of the hillslope. This correction assumes that the surface is smooth whereas the rainfall flux onto a hillslope with a rough surface will also vary according to the ratio of the curvature of the roughness elements to the drop size. We do not explicitly account for the effect of surface roughness

on the rainfall flux and we recognize that its effects will be incorporated into the calibration procedure.

[4] Substituting (1) into the familiar equation for kinetic energy, kinetic energy per unit area (E_k) is expressed as

$$E_k = \frac{\rho i v^2 \cos \theta}{2}, \quad (2)$$

where v is raindrop velocity (m s^{-1}). However, on a vegetated surface, raindrop impacts can be suppressed by vegetation. In grasslands, raindrops intercepted by vegetation have essentially zero velocity upon reaching the soil surface and thus have no capacity to detach sediment. Therefore C_v is introduced into (2) to yield an effective kinetic energy (E'_k),

$$E'_k = \frac{\rho i v^2 (1 - C_v) \cos \theta}{2} \quad (3)$$

where C_v represents the proportion of area covered by ground-level vegetation. Rain power (R , W m^{-2}) is then

$$R = \frac{dE'_k}{dt} = \frac{\rho i v^2 (1 - C_v) \cos \theta}{2}. \quad (4)$$

[5] Many studies have concluded that a layer of water on the soil surface also attenuates the erosive effect of raindrop impact [Palmer, 1946; Moss and Green, 1983; Mutchler and McGregor, 1983; Schultz et al., 1985; Kinnell, 1991, 1993a]. Several of these have found that the erosive effect is dependent on the ratio between flow depth and raindrop diameter [Palmer, 1946; Moss and Green, 1983; Kinnell, 1991, 1993a]. To account for the attenuation of detachment rates by water on the soil surface, we introduce a function, $A(h, d)$, that varies between 0 and 1 so that

$$\psi = \alpha R^\beta A(h, d), \quad (5)$$

where ψ ($\text{g m}^{-2} \text{s}^{-1}$) is sediment detachment rate per unit area, α and β are empirically determined constants, h is flow depth, and d is raindrop diameter. The function, $A(h, d)$, is conceptually similar to one proposed by Kinnell [1993a], although Kinnell's also accounts for the effect of flow depth on sediment transport.

[6] Determining the correct relationship between flow depth, drop size, and sediment detachment is critical for deriving the attenuation function. Palmer [1965] found that the maximum forces from raindrop impact on a surface occurred when a drop falls into a thin layer of water. Mutchler and McGregor [1983] investigated the effect of flow depths on erosion rates during rainfall simulations and concluded that erosion rate decreases with increasing flow depths but their experiments were limited to $h/d > 2$. To our knowledge there have been only two studies that specifically investigated the detachment of sediment by drop impact through a range of water depths. McCarthy [1980] found that the volume of sediment detached declines exponentially with increasing h/d so that detachment is greatest with no water on the surface. Similarly, Schultz et al. [1985] determined that sediment detachment decreases exponentially with increasing water depths. An important

caveat to these two studies is that they were both conducted with ponded water. A moving water layer could affect these results, especially in the case of turbulent flow.

[7] Following the results of McCarthy [1980] and Schultz et al. [1985], we assume that detachment declines exponentially with water depth. Whereas McCarthy [1980] used sand in his experiments, Schultz et al. [1985] used a cohesive soil which is more similar to the soils in our study, therefore we use their data. Nondimensionalizing their results [Schultz et al., 1985] yields

$$\frac{\psi}{\psi_0} = e^{-1.8h/d}, \quad (6)$$

where ψ_0 is the detachment rate with no water on the surface. Schultz et al. [1985] used a single drop size (1.6 mm diameter) in their experiments so, due to the paucity of appropriate data, we must extrapolate their results to apply to a range of drop sizes. This assumes an approximately consistent interaction between h/d and sediment detachment, which may not be correct.

[8] For an ideal sheet flow (i.e., uniform flow depth), (6) may be used for the attenuation function so that (5) becomes

$$\psi = \alpha R^\beta e^{-1.8h/d}. \quad (7)$$

However, surface runoff is typically composed of different threads of flow producing an across-slope distribution of flow depths [Emmett, 1970; Dunne and Dietrich, 1980; Morgan, 1980; Abrahams et al., 1989]. In this case, (7) is modified so that the various flow depths (h_1, h_2, \dots, h_n) are represented such that

$$\psi = P(h_1)\alpha R^\beta e^{-1.8h_1/d} + P(h_2)\alpha R^\beta e^{-1.8h_2/d} + \dots + P(h_n)\alpha R^\beta e^{-1.8h_n/d} \quad (8)$$

or

$$\psi = \alpha R^\beta \sum_{h=0}^{3d} P(h) e^{-1.8h/d}, \quad (9)$$

so, from (5), the attenuation function becomes

$$A(\bar{h}, d) = \sum_{h=0}^{3d} P(h) e^{-1.8h/d}, \quad (10)$$

where $P(h)$ is the proportional area covered by a flow depth h . Equation (9) therefore explicitly considers the spatial distribution of across-slope flow depths in modulating detachment rates by rain power. Flow depths greater than 3 drop diameters are not considered because raindrop impact is relatively nonerosive beyond this threshold [Moss and Green, 1983; Kinnell, 1990, 1991, 1993a]. A similar, albeit simpler, approach was followed by Parsons and Abrahams [1992] to examine the effect of flow depth distributions on sediment detachment.

[9] This paper consists of two sections. In the first, we present results from a series of rainfall simulation experiments designed to determine whether rain power may be useful for predicting sediment detachment rates. As shown by (9), this requires observations regarding flow depth distributions. In the second section, we demonstrate how

the results from the experiments may be incorporated into a numerical model for determining sediment discharge from entire lengths of hillslopes.

2. Materials and Methods

2.1. Field Site

[10] The fieldwork for this study was carried out at Sedgwick Reserve, a University of California natural reserve, near Santa Barbara, California. The reserve is located on the margins of the Santa Ynez Valley, in the tectonically-active Transverse Ranges. The climate is semi-arid Mediterranean with an average annual rainfall of 50 cm. The landscape is dominated by short (80–100 m), steep rolling hillslopes underlain by the Paso Robles Formation, a Pliocene conglomerate [Dibblee, 1993]. The soil is a silty clay loam [Shipman, 1972] with shrink-swell clays indicated by many large cracks during the dry season. The soil surface has significant microtopography from hoofprints, burrowing mammals [Gabet, 2000], shrink-swell motion, and root growth, with relief occasionally reaching 2 cm. Hillslopes gentler than 30° were cleared of native vegetation for cattle grazing during the late nineteenth century and are presently vegetated by exotic, annual grasses (*Avena* and *Bromus*). Grazing continues, although at relatively low stocking rates (40 cow days ha⁻¹ y⁻¹).

2.2. Experimental Plots

[11] Eleven plots were used throughout the field site to sample a range of hillslope angles (4°–17°) and ground cover densities (18–94%). A pin frame with 10 cm resolution was used to estimate the ground cover density which included live vegetation and litter. During the series of experiments on each plot, the ground cover was gradually reduced by clipping vegetation and carefully removing litter.

2.3. Rainfall Simulations

[12] Forty-four rainfall simulation experiments were performed using a portable rainfall simulator over 6 m × 2.4 m plots. The simulator is a version of the model described by Dunne *et al.* [1991] and has nozzles moving back and forth along two parallel tracks. The nozzles used were the Delavan SQ72 and SQ150. Drop size distributions at different intensities were measured using the flour pellet method [Carter *et al.*, 1974] and median drop sizes ranged from 1.9 mm to 3.9 mm. The flour pellet method, however, only samples the rainfall for about 1 second so there is an assumption that the results represent the time-averaged distribution of drop sizes [Salles *et al.*, 1999]. Impact velocities of the median drop sizes for each run were determined with the technique described by Iverson [1980] using data from Laws [1941] and were calculated to reach 91–95% of terminal velocities. Rainfall intensities, held constant during each run, varied between experiments from 5 to 13 cm hr⁻¹. Although fewer than 3% of the recorded 1-hr intensities in the region are greater than 2 cm hr⁻¹ (NOAA, Figueroa Mountain Ranger Station), short bursts of rainfall with intensities in this range are not uncommon. Each experiment lasted 30–50 min.

[13] Timed, 1-liter samples of runoff were collected from a trough at the bottom of the plot. The elapsed time between samples varied from 2–4 min to guarantee that the sampling was not in phase with the pulsatory rainfall. The time

necessary to fill the 1-liter bottle was generally longer than several cycles of the rainfall pulse, which should have also reduced the effects of the pulsatory rainfall. The samples were filtered, dried, and weighed to measure sediment discharge. The runoff and sediment were also analyzed for carbon and nitrogen concentrations; these results are presented and discussed by Fierer and Gabet [2002].

2.4. Flow Simulations

[14] Eleven experiments were performed to measure sediment detachment caused solely by flow. In these, water was spread across the uphill end of the plot from a perforated pipe. Discharges were adjusted to approximately match the discharges measured in the rainfall simulations. Because of infiltration, the discharge from the perforated pipe was greater than the discharge at the bottom of the plot resulting, perhaps, in greater sediment detachment at the top of the plot. Runoff samples were taken and analyzed as in the rainfall simulations.

2.5. Depth Measurements

[15] When the flow simulations attained steady state discharge, flow depth measurements were taken along a cross section perpendicular to the flow approximately 0.75 m uphill of the trough (to avoid drawdown effects from the flow cascading over the lip of the trough). Depth was measured every 10 cm across the plot with a thin ruler. Measurements were read to 1 mm precision, however, difficulties in accurately reading the ruler as well as flow disturbance from the ruler itself introduced errors estimated to be about ±1 mm.

3. Results

3.1. Flow Depths

[16] In the initial moments of the rainfall simulations, water collected in depressions on the soil surface. As each depression filled from direct rainfall and flow from upslope, water overtopped the lip of the depression and cascaded to the next depression, in a manner reminiscent of step-pool morphology in rivers. At steady state flow, all the pools were connected and contributing discharge. Three different types of flow could be identified throughout the plot. The first type was the slow-moving flow in the deep (10–15 mm) pools. The second was the shallower (4–8 mm), quicker threads of flow linking the pools. The third was the very shallow (1–2 mm) flow that occupied the rest of the plot.

[17] From Figure 1, the depth distribution data indicate a linear relationship ($n = 10$, $R^2 = 0.58$, $p < 0.05$) between mean depth 0.75 m upslope of the trough (\bar{h} , cm) and unit discharge (q , cm² s⁻¹),

$$\bar{h} = 0.8q + 2.9. \quad (11)$$

The relationship predicts nonzero flow depths when there is no flow because of the microtopography that produces significant ponding. At the scale of the plot, microtopography is a strong influence on mean flow depth. At the hillslope scale, however, we would expect that vegetation density would become an important factor in controlling mean flow depth by increasing the surface roughness.

[18] Despite the imprecision in measuring flow depths, the distribution of across-slope depths follow approximately a Poisson distribution (Figures 2a and 2b). The Poisson

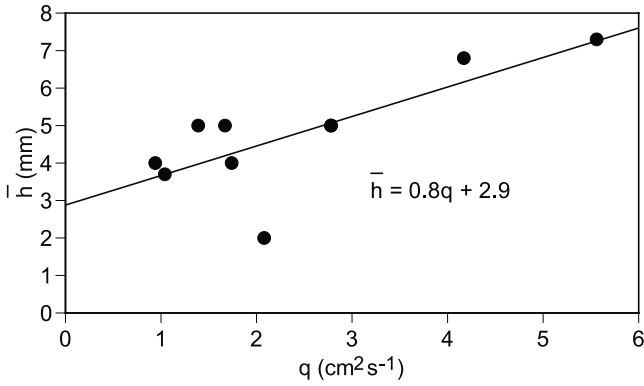


Figure 1. Data relating mean flow depth to unit discharge. $R^2 = 0.58$.

distribution is a discrete distribution, and thus flow depth values can only be represented as integers. However, at the scale of measurement and computation (mm), the functional difference between a continuous and discrete distribution is negligible. The Poisson distribution requires only one parameter, the mean [Krumbein and Graybill, 1965], so that

$$P(h) = \frac{\bar{h}^h e^{-\bar{h}}}{h!}, \quad (12)$$

where $P(h)$ is the proportional area covered by a depth h and \bar{h} is the mean depth. Abrahams *et al.* [1989] found that

flow depths on natural hillslopes followed a negative exponential distribution at unit discharges ($0.3\text{--}0.4 \text{ cm}^2 \text{ s}^{-1}$) lower than those reported here. This agrees well with our results because a negative exponential distribution resembles a Poisson distribution when the mean depth is low. Incorporating (12) into (10), the function describing the attenuation of detachment rates with increasing flow depth is expressed as

$$A(\bar{h}, d) = \sum_{h=0}^{3d} \frac{\bar{h}^h e^{-\bar{h}}}{h!} e^{-1.8h/d}. \quad (13)$$

For example, consider a situation where 3 mm drops are impacting a flow with a unit discharge of $0.8 \text{ cm}^2 \text{ s}^{-1}$. The Poisson distribution of flow depths can be determined with the average flow depth calculated from (11). Figures 3a and 3b demonstrate how the distribution of depths is combined with the exponential decline in detachment rates to determine the value of $A(\bar{h}, d)$ for this particular combination of unit discharge and drop size. Values for the attenuation function are shown for a range of discharges in Figure 4.

3.2. Sediment Detachment and Transport

[19] Sediment concentrations from samples taken during steady flow were averaged for each run. In general, the standard deviation of the sediment concentrations during the rainfall simulations was approximately 10–20%, suggesting

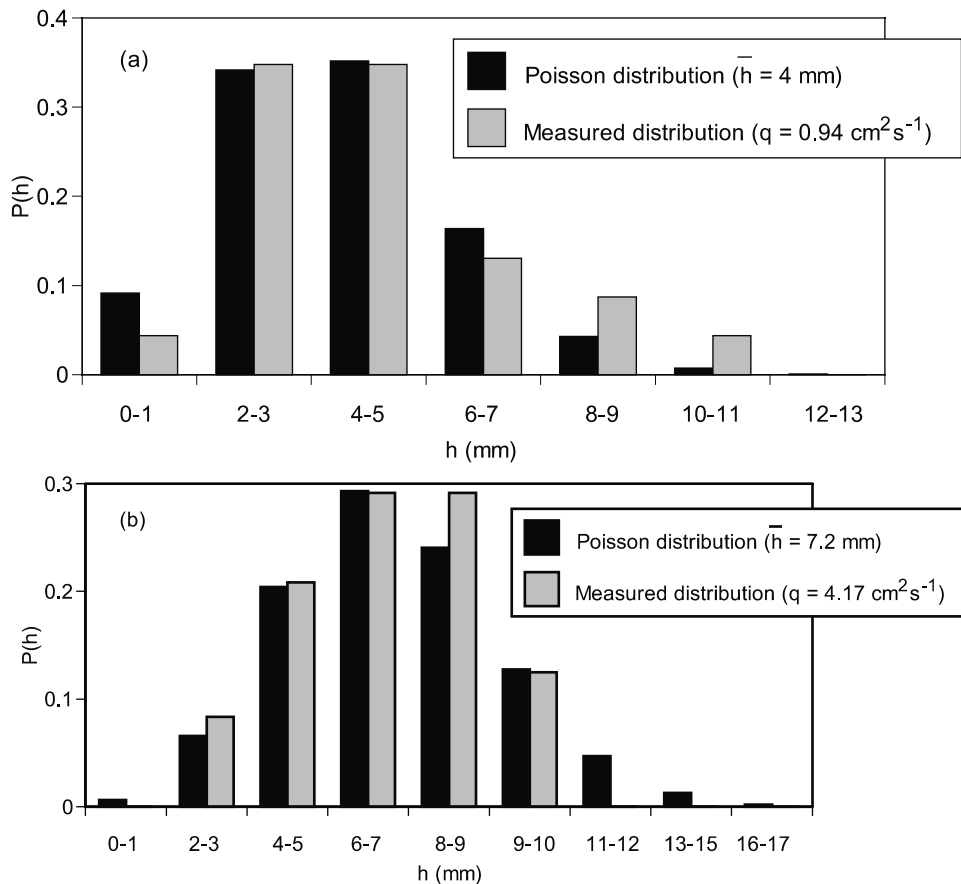


Figure 2. (a) Measured flow depth distribution for a unit discharge of $0.94 \text{ cm}^2 \text{ s}^{-1}$ compared to the Poisson distribution (χ^2 test; $P > 0.25$). (b) Measured flow depth distribution for a unit discharge of $4.17 \text{ cm}^2 \text{ s}^{-1}$ compared to the Poisson distribution (χ^2 test; $P > 0.75$).

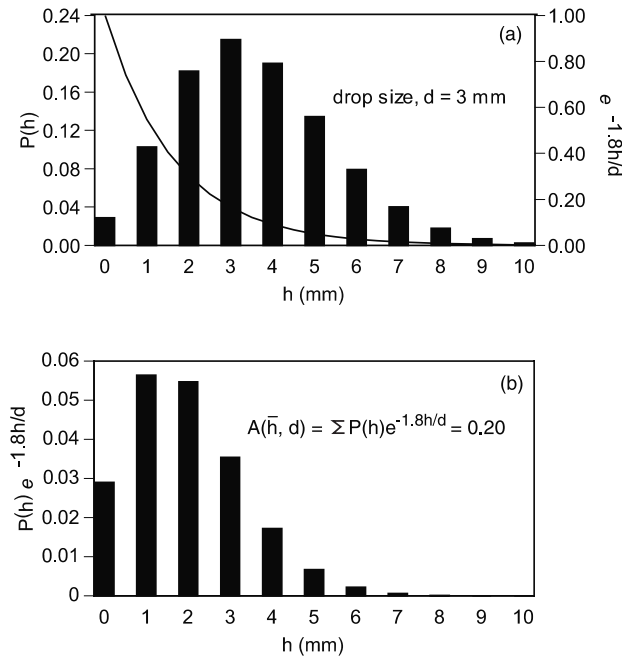


Figure 3. (a) Bar graph is the Poisson distribution of flow depths for a unit discharge of $0.8 \text{ cm}^2 \text{ s}^{-1}$. Line graph is the exponential decline of detachment rates when drop size, d , is 3 mm. (b) Calculation of the attenuation function for this combination of unit discharge and drop size.

that the pulsatory rainfall may have had an effect on sediment transport in the plots. Sediment concentrations were several orders of magnitude higher in the rainfall simulations than in the flow simulations (Figure 5). Compared to raindrop impact, therefore the flow is inefficient in detaching sediment from these cohesive soils. Hudson [1957] and Young and Wiersma [1973] came to similar conclusions in studies where the effect of raindrop impact was suppressed by screens installed just above the soil surface. Shallow flows are particularly inefficient in detaching sediment from clay-rich soils [Ellison, 1947].

[20] Over the length of the plot, the step-pool flow efficiently sorted the detached sediment. Coarse material was transported as bed load or by raindrop-induced flow transport [Kinnell, 1988, 1990, 1991; Kinnell and Wood, 1992] but quickly became trapped in the depressions, leaving a thin lag deposit of sand and fine gravel where flow velocities were slower and the greater flow depths protected it from resuspension by drop impact. In contrast, the finer material remained suspended and was carried the length of the plot. This microtopography-induced selective transport was effective enough that 90% of the sediment collected in the runoff was typically finer than $53 \mu\text{m}$ and Rouse calculations [Reid and Dunne, 1996] indicate that this size fraction was transported as wash load. Over time, this selective transport might be expected to armor the soil surface, leading to decreased rates of detachment, however high rates of bioturbation by cattle and burrowing mammals [Gabet, 2000] prevent any surface coarsening.

[21] Since the sediment transported off the plot is primarily wash load, steady state sediment discharge per unit contour width of slope (q_s) at any point x is simply the

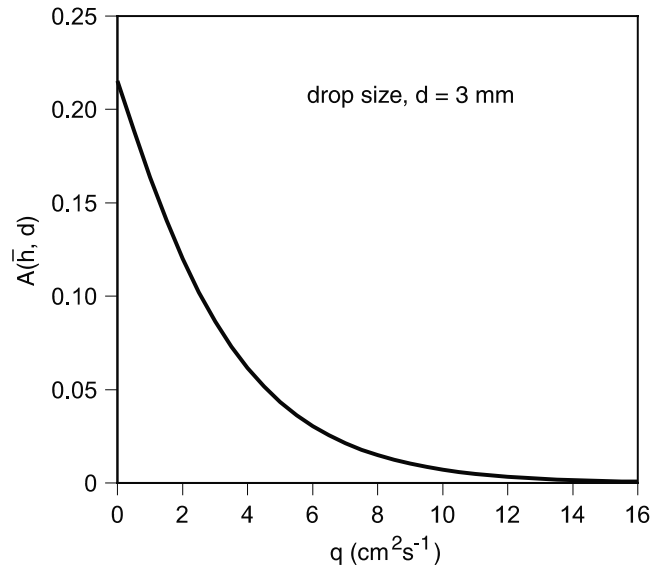


Figure 4. Values of the attenuation function for a range of unit discharges and a raindrop diameter of 3 mm. Although, theoretically, the maximum value of $A(\bar{h}, d)$ should be unity, ponded water will suppress detachment rates even when there is no flow.

total of the sediment detachment rates from the upslope contributing area,

$$q_s = \sum_0^x \psi(x) \Delta x, \quad (14)$$

where ψ depends on the distance from the divide because of the downslope increase in flow depths during rainfall events. Note that ψ should be considered a “wash load” detachment rate because only the wash load portion of the sediment detached is carried a significant distance. Parsons and Abrahams [1992] have also observed that only a fraction of sediment detached is removed by overland flow.

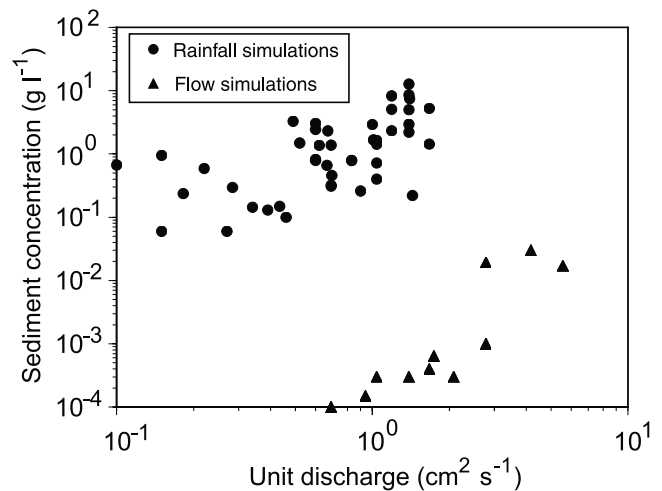


Figure 5. Sediment concentrations versus unit discharge generated with and without rainfall. The significantly higher sediment concentrations during the simulations with rainfall indicate that drop impact detaches sediment much more effectively than the flow.

Table 1. Rainfall Simulation Experiments

Run	i , cm hr ⁻¹	q_s , cm ² s ⁻¹	θ , deg	C_v	v (m s ⁻¹)	R (W m ⁻²)	$A(\bar{h}, d)$	$q_s \times 10^{-5}$ g m ⁻¹ s ⁻¹
1	6.9	0.34	10	0.94	6.5	0.024	0.81	4.90
2	12.5	1.40	10	0.94	7.5	0.058	1.39	56.0
3	6.5	0.46	10	0.88	6.3	0.042	0.63	4.6
4	10.1	1.04	10	0.88	7.6	0.096	1.58	27.0
5	6.0	0.60	17	0.72	6.3	0.088	0.62	49.2
6	12.1	1.39	17	0.72	7.6	0.260	1.52	307.2
7	6.2	0.60	17	0.72	6.3	0.091	0.62	47.4
8	11.7	1.39	17	0.72	7.6	0.250	1.52	410.1
9	6.0	0.10	14	0.86	6.3	0.045	0.66	6.7
10	11.1	0.69	14	0.86	7.6	0.121	1.64	95.2
11	5.1	0.22	14	0.68	6.7	0.099	1.29	13.0
12	11.9	1.01	14	0.68	7.4	0.281	1.41	168.7
13	5.5	0.39	4	0.98	6.7	0.007	1.28	5.1
14	5.0	0.15	4	0.98	6.7	0.006	1.30	0.9
15	6.0	0.27	4	0.98	6.3	0.007	0.65	1.6
16	7.4	1.04	17	0.82	6.5	0.075	0.72	74.9
17	5.5	0.83	17	0.74	6.3	0.075	1.32	65.6
18	5.5	0.83	17	0.66	6.7	0.112	1.20	65.6
19	4.5	0.15	13	0.70	6.5	0.076	0.83	14.3
20	11.0	1.00	13	0.70	7.5	0.250	1.46	292.0
21	12.5	1.19	13	0.56	7.5	0.417	1.42	277.3
22	10.5	1.04	9	0.74	6.5	0.158	1.45	170.6
23	9.7	1.04	9	0.64	7.6	0.277	1.50	148.4
24	7.3	0.69	9	0.68	6.5	0.136	0.76	21.4
25	6.6	0.52	13	0.64	6.5	0.136	0.79	77.5
26	8.2	0.62	13	0.62	6.5	0.177	0.77	84.9
27	11.0	1.19	13	0.62	7.5	0.319	1.42	604.5
28	6.8	0.60	13	0.39	6.4	0.229	0.72	146.4
29	10.1	1.19	13	0.35	7.6	0.513	1.55	984.1
30	7.3	0.60	13	0.32	6.5	0.283	0.77	183.0
31	11.6	1.40	13	0.32	7.5	0.600	1.39	1048.6
32	6.7	0.67	13	0.34	6.5	0.253	0.76	155.4
33	11.1	1.39	13	0.34	7.6	0.572	1.43	1192.6
34	7.4	0.49	13	0.34	7.5	0.372	1.55	161.2
35	11.3	1.39	13	0.34	7.6	0.581	1.43	1765.3
36	6.7	0.69	5	0.86	6.5	0.055	0.76	22.1
37	13.3	1.67	5	0.76	7.5	0.249	1.35	238.8
38	12.0	1.39	5	0.52	7.5	0.448	1.43	695.0
39	12.2	1.67	5	0.45	7.5	0.523	1.35	876.8
40	12.2	1.39	5	0.46	7.5	0.514	1.39	760.3
41	13.0	1.04	11	0.18	7.5	0.819	1.45	2459.6
42	14.6	1.19	11	0.18	7.5	0.917	1.42	2378.8
43	13.1	0.76	11	0.51	7.5	0.490	1.50	871.0
44	12.3	1.19	11	0.46	7.5	0.511	1.42	1807.6

Substituting (5) into (14), sediment discharge is determined with

$$q_s = \alpha R^\beta \sum_0^x A(\bar{h}, d) \Delta x, \quad (15)$$

where $A(\bar{h}, d)$ defined in (13). To estimate values for α and β with the data from the rainfall simulation experiments (Table 1), (15) is rearranged as

$$\frac{q_s}{\sum_0^x A(\bar{h}, d) \Delta x} = \alpha R^\beta, \quad (16)$$

where R is calculated according to (4), steady state q_s was measured during the experiments, and x is the plot length (6 m). To calculate $\sum A(\bar{h}, d)$ along the length of the plot with (13) at steady state, unit discharge (q) can be determined at any distance x along the length of the plot with

$$q = (i - f)x, \quad (17)$$

where f is infiltration capacity. Unit discharge was calculated along the length of the plot for each experiment and combined with (11) and (13) to determine values for $A(\bar{h}, d)$ at a Δx of 1 m. We only consider the median drop size (by volume) in determining the value of the attenuation function and the velocity of the raindrops although *Parsons and Gadian* [2000] have proposed that using a single drop size to represent the entire drop size distribution may not be appropriate. Potential errors introduced by the use of the median drop size are discussed later.

[22] Figure 6 shows a significant relationship ($n = 44$, $R^2 = 0.88$, $p < 0.005$) between rain power and the left-hand side of (16) such that

$$\psi = 0.011R^{1.4}A(\bar{h}, d). \quad (18)$$

This indicates that rain power predicts reasonably well sediment detachment rates of wash load material by raindrop impact for the steep rangeland slopes studied here. This result also suggests that using the median drop

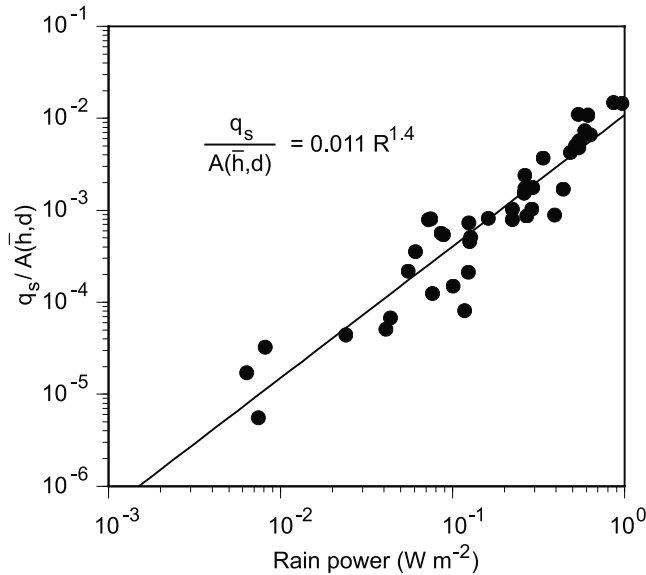


Figure 6. Calibration of the rain power formulation. $R^2 = 0.88$.

diameter is adequate although our approach could be modified to incorporate a probability distribution of drop sizes. Equation (18) can be generalized to apply to natural rainfall conditions. By combining a relationship between the terminal velocity of raindrops and drop diameter [Gunn and Kinzer, 1949]

$$v = 5.1d^{0.4}, \quad (19)$$

with a relationship between median drop diameter and rainfall intensity (cm h^{-1}), [Laws and Parsons, 1943]

$$d_{50} = 1.88i^{0.182}, \quad (20)$$

the velocity of the d_{50} can be expressed as a function of intensity [Schmidt, 1993]

$$v = 6.6i^{0.07}. \quad (21)$$

Equation (21) can be inserted into (4) and (18) so that the rate of detachment for natural rainfall can be predicted with

$$\psi = 1.9 \times 10^{-4} i^{1.6} [(1 - C_v) \cos \theta]^{1.4} A(\bar{h}, d). \quad (22)$$

Note that in (22) the units of intensity have been converted from (m s^{-1}) to (cm h^{-1}), a more common measure of rainfall intensity.

3.3. Flow Resistance Coefficient

[23] Measures of hydraulic resistance were needed for the modeling portion of this investigation but, because of the complex nature of the flow, they could not be determined directly from flow depth and velocity measurements. Instead, flow resistance coefficients spatially averaged over the entire plot, expressed as effective Manning's n values, were estimated by fitting a kinematic wave model to the recession limb of the hydrographs from the rainfall experiments (see Appendix A for details). Although the use of Manning's equation assumes turbulent flow, previous studies [Roels, 1984; Engman, 1986] have shown that this may be reasonable for rangelands. Additionally, even at Rey-

nold's numbers < 1000 , raindrop impact would have induced turbulence in the flow [Dunne and Dietrich, 1980; Rouhipour et al., 1999]. Figure 7 presents a relationship ($n = 24$, $R^2 = 0.60$, $p < 0.005$) between an effective Manning's n and C_v where

$$n = 0.053e^{2.7C_v}. \quad (23)$$

The values for Manning's n determined here agree with the range of values found by others [Palmer, 1946; Engman, 1986] for grazed grasslands. The significant microtopography on the soil surface likely accounts for much of the roughness represented by the Manning's n values. However, since the roughness caused by the microtopography is spatially constant, differences in the total roughness caused by different values of C_v can be discerned.

[24] Although Rouhipour et al. [1999] found that Manning's equation performed better than the Darcy-Weisbach equation in predicting flow velocity in surface runoff even when the flow was not turbulent, we would have preferred to express the flow resistance as a Darcy-Weisbach friction factor [e.g., Abrahams and Parsons, 1991] because it accounts for the dependency of flow resistance on flow depth. In the case of overland flow, the depth of the flow relative to the height of the surface asperities may strongly affect flow resistance [Abrahams et al., 1992; Gilley et al., 1992]. Unfortunately, measuring the necessary flow characteristics at the scale required for accurately determining the Darcy-Weisbach friction factor was not feasible, particularly since the nature of the flow changed continuously along the length of the plot.

4. Discussion

[25] Simulating rainfall over large plots on steep slopes requires the use of a rainfall simulator with nozzles that spray water across the plot. Because these nozzles are designed for agricultural purposes, the pressure needed to achieve an even distribution of rainfall and to accelerate the raindrops up to terminal velocity results in unnaturally high rainfall intensities. To reduce the intensities, several methods have been devised to average the intensity in time or space, with the result that the rainfall is pulsed [Kinnell, 1993b]. The two-track simulator used here [Dunne et al., 1991] covers

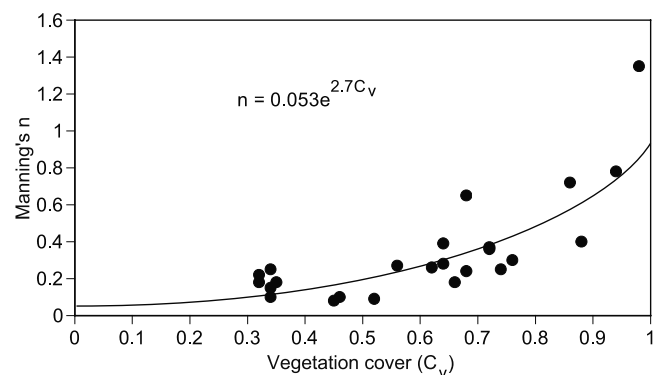


Figure 7. Effective Manning's n versus proportional area covered by vegetation (C_v). Values for Manning's n were determined from the recession limbs of hydrographs measured during the flow simulation experiments. $R^2 = 0.60$.

approximately two-thirds of the plot with rainfall at any instant. The length of time that any part of the plot is not receiving rain is dependent on the speed at which the nozzles are moving along the tracks. The maximum instantaneous intensity on the plot therefore may be 50% greater than the average intensity and the degree to which this difference will have an effect depends, in part, on the exponent β in (16). If β is unity, this difference will have no effect but as β increases beyond unity, the results from the pulsed rainfall simulations will overpredict values for both α and β under natural rainfall. The amount of overprediction is unquantifiable because of the confounding effect of flow depths, however the value for β found here, 1.4, may be similar enough to unity to suggest that the error may not be large.

[26] In addition to experimental constraints, there are three other limitations that merit discussion. First, the attenuation function, $A(h, d)$, is based on the poorly-understood relationship between sediment detachment, flow depth, and drop size. Work by *Palmer* [1965] suggests that the maximum detachment by drop impact should occur in a thin layer of water but others [*McCarthy*, 1980; *Schultz et al.*, 1985] have found that the maximum detachment occurs with no water on the surface. Because a portion of the landscape is generally covered only by very thin flows during runoff-generating rainstorms, the predicted sediment detachment will be sensitive to how the attenuation function is parameterized. Second, whereas we found that the across-slope distribution of flow depths could be approximated by a Poisson distribution, flow depth distributions may vary from one landscape to the next. Third, the nonlinear dependence of sediment detachment rates on both the attenuation function and the drop velocity suggests that using the d_{50} , in this case, may introduce some errors. If the drop sizes are normally distributed by volume, using the d_{50} does not produce any errors in either the rain power calculation or the attenuation function. As the distribution becomes skewed, however, errors appear. For example, using the d_{50} , rather than the entire drop size distribution reported by *Jayawardena and Rezaur* [2000] for a typical rainstorm, will underestimate the rain power value by 12% and the attenuation function by 16% (for a unit discharge of $2 \text{ cm}^2 \text{ s}^{-1}$). The distributions for the experiments presented here exhibit both left and right skewness, depending on the nozzle used. The difficulty with using the entire distribution for the experiments lies in the determination of the velocities of each drop size at impact.

[27] The three limitations presented above emphasize the utility of our approach, rather than detract from it. Because the attenuation function and the flow depth probability distribution function are explicitly considered in (13), they can be easily replaced by others when applied to different landscapes or as more data become available. Additionally, rain power can be calculated for each drop size in natural rainstorms where it can be assumed that all drop sizes have reached terminal velocity.

[28] With these caveats, our results agree with similar equations that include rainfall intensity as a variable in predicting sediment detachment by raindrop impact. With slope and vegetation cover held constant, (22) indicates that sediment detachment rate is proportional to $i^{1.6}$. The exponent, 1.6, is similar to values found by others; *Ekern* [1954] determined that the “erosivity” of raindrop impact was

proportional to $i^{1.5}$, and *Meyer* [1981] concluded that interrill erosion by raindrops was proportional to $i^{1.6}$ for cohesive soils.

[29] Because sediment detachment is primarily by raindrop impact in this landscape, the formation of rills will be suppressed. The soil surface underneath deeper threads of flow are protected from raindrop detachment while the rest of the soil surface erodes. This results in an essentially diffusive process where high points in the microtopography are smoothed out [*Dunne and Aubry*, 1986]. An absence of rills on the short hillslopes at Sedgwick Reserve supports this conclusion. On longer hillslopes, detachment from the flow may overwhelm detachment by raindrops at some critical distance from the divide and rills should form. Over time, other diffusive processes, such as bioturbation, will also inhibit rill formation.

5. Model

5.1. Sediment Detachment

[30] In this section, we demonstrate a modeling approach to calculate sediment detachment and discharge of fine-grained particles over the length of a hillslope. Determining rates of sediment detachment by rain power during rainstorms requires a prediction of downslope and across-slope variations in flow depths. Downslope variations in discharge and flow depths are determined with the kinematic wave approximation [*Henderson and Wooding*, 1964; *Woolhiser*, 1975] which assumes that the water surface slope is parallel to the hillslope gradient. On a planar hillslope, the one-dimensional continuity equation

$$\frac{\partial q}{\partial x} + \frac{\partial \bar{h}}{\partial t} = i - f, \quad (24)$$

where f is infiltration capacity, is coupled with Manning’s equation

$$q = \frac{s^{0.5} \bar{h}^{1.67}}{n}, \quad (25)$$

where s is hillslope gradient and n is a function of C_s (23). The flow routing does not explicitly recognize the distribution of flow depths so (24) and (25) only consider mean flow depth. The term \bar{h} in (24) is calculated with the Lax-Wendroff finite-difference scheme [*Lima*, 1993] with a 1-m mesh size and a 1-s time step. The value of $A(\bar{h}, d)$ is then calculated at each node along the length of the slope with (13). The detachment rate of the wash load material at each node is calculated with (22) at one minute intervals of model-time and stored in a 2-dimensional matrix, producing a space-time map of detachment rates (see later).

5.2. Sediment Discharge

[31] Ultimately, we are modeling sediment detachment because we are interested in the delivery of sediment from rangelands to address water quality concerns. The landscape characteristics of our field site, specifically the gradients and the fine texture of the sediment in transport, allow us to adopt a simplified approach to estimating sediment discharge from overland flow. First, raindrop impact is the dominant form of detachment (Figure 5); therefore the role of the flow in detaching sediment can be disregarded. Second, because of the microtopography, the sediment transported beyond the

Table 2. Model Parameters

Model Run	1	2
Duration (hr)	1	1
Precipitation intensity (cm hr ⁻¹)	1.5	1.5
Infiltration capacity (cm hr ⁻¹)	0.5	0.5
Hillslope length (m)	100	100
Slope angle (°)	15	15
Vegetation cover (C _v)	0.80	0.40

small pools is primarily wash load. Third, the hillslopes are short and steep. This last condition suggests that the material transported as wash load will not be redeposited. Where these conditions are not met, (22) would need to be incorporated into a more complex set of equations [e.g., *Foster and Meyer, 1975; Hairsine and Rose, 1992*].

[32] Modeling sediment discharge in the situation described above presents a challenge because detachment rates change spatially and temporally so that sediment discharge is a function of the space-time trajectory of the flow. This requires a Lagrangian approach that can be implemented through the use of the method of characteristics to solve (24) coupled with (25). With this method, discharge can be calculated analytically along a curve (a characteristic) in

the $x-t$ plane [*Henderson and Wooding, 1964; Woolhiser and Liggett, 1967; Dunne and Dietrich, 1980*]. To determine the path of a characteristic in the $x-t$ plane, equation (8) from *Dunne and Dietrich [1980]*, is rewritten as

$$t = \left[\frac{x - x^0}{\alpha(i - f)^{m-1}} \right]^{1/m}, \quad (26)$$

where t is elapsed time since the start of precipitation, x is the position of the characteristic at t , and the other variables are explained in Appendix A. At $t = 0$, an initial position, x^0 , is specified along the length of the slope. The time t for the position of the characteristic at any x can then be solved, thus defining the space-time path of the characteristic that originated at x^0 .

[33] To calculate sediment discharge, characteristic trajectories are determined for initial positions spaced at 1-m intervals along the length of a planar slope (hillslope characteristics are given in Table 2). The path of each characteristic is then “superimposed” over the space-time map of detachment rates (see Figures 8a and 8b). Sediment discharge (q_s) from the base of the slope is the sum of the detachment rates encountered by each characteristic or

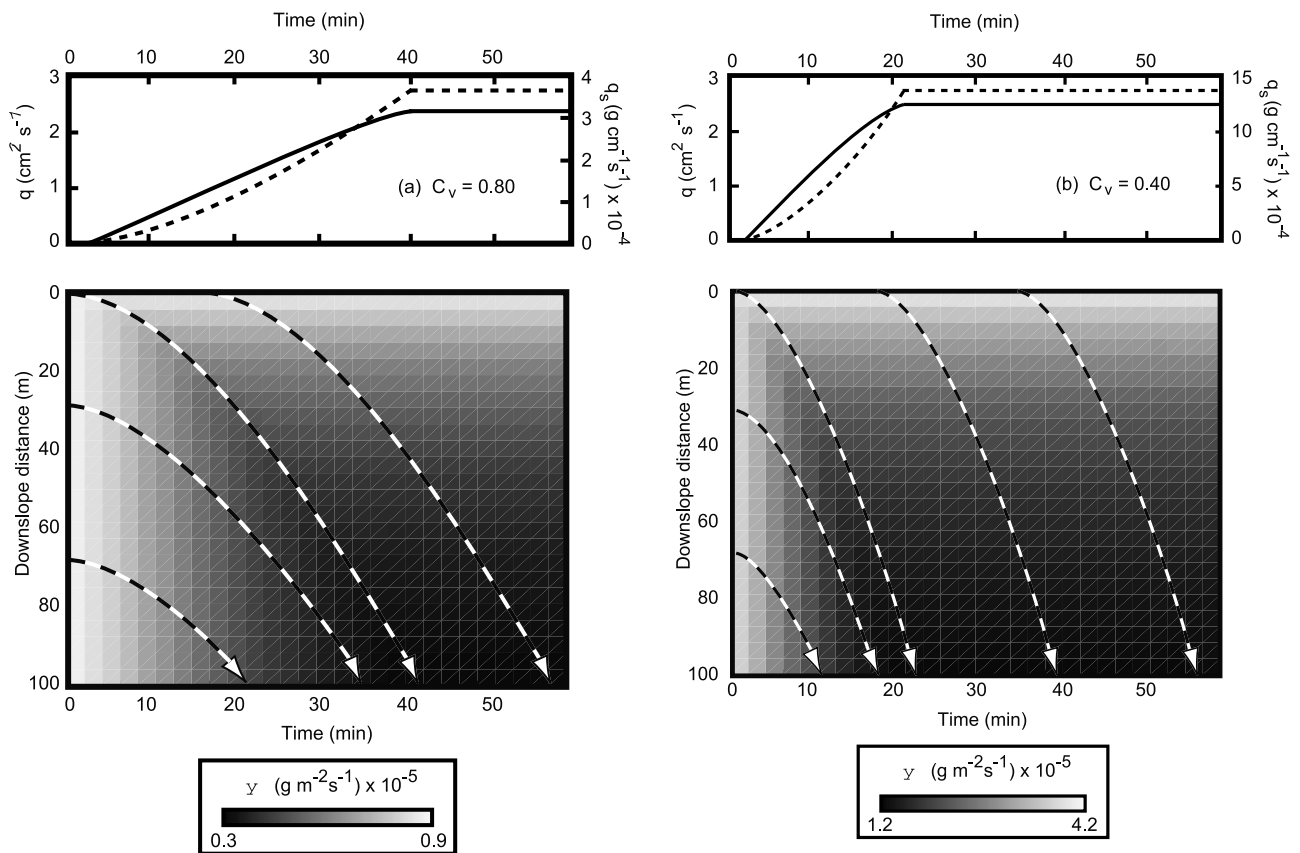


Figure 8. Results from two model runs. Initial conditions are identical except for the values of C_v , which is 0.80 for Figure 8a and 0.40 for Figure 8b. The upper graph is the hydrograph (dashed line) and sedigraph (solid line) from the bottom of the slope. The lower graph shows the spatial and temporal distribution of detachment rates. Each column displays detachment rates along the length of the hillslope at the specified time. The lighter colors represent areas of high detachment rates while the darker areas have lower detachment rates. Several characteristic trajectories are shown as dashed lines with arrows. Sediment discharge is the sum of the detachment rates encountered by each characteristic. Note that Figures 8a and 8b have different scales for sediment discharge and detachment rates.

$$q_s = \sum_{x^0}^L \psi(x, t) \Delta x, \quad (27)$$

where L is the length of the slope. As previously mentioned, this assumes that all of the sediment transported is wash load and that none of it settles out. Calculating sediment delivery in this fashion is not appropriate where deposition of sediment along the length of the hillslope is important [Foster and Meyer, 1975].

5.3. Modeling Results

[34] Table 2 lists the parameters for two model runs. Except for the values of C_v , the conditions for the runs are identical. The modeled rainfall intensity, 1.5 cm hr^{-1} , has a 2-year recurrence interval for the field site. Figures 8a and 8b illustrate the spatial and temporal changes in detachment rates. In the first moments of the storm, detachment is high and uniform along the length of the slope. As the rainstorm progresses and flow depths increase, detachment rates decrease along the length of the slope, eventually reaching a minimum near the base of the slope where the combination of flow depths and vegetation cover suppresses the detachment of soil particles. Gilley *et al.* [1985] modeled a similar downslope decrease in detachment rates caused by increasing flow depths.

[35] The importance of vegetation cover in controlling detachment rates can be seen by comparing Figures 8a and 8b. With the sparser vegetation cover, there is a five-fold increase in the maximum detachment rate and a four-fold increase in steady state sediment discharge. The vegetation cover also has a significant effect on the flow. Because the hydraulic roughness depends on C_v , hillslopes with less vegetation will convey flow more efficiently. For example, run 2 (Figure 8b) reaches steady state flow 20 min sooner than run 1, indicating that the area contributing sediment to the base of the slope is expanding faster. Decreases in vegetation cover therefore result in higher rates of sediment detachment and quicker hydrological response times.

[36] Whereas rain power increases rapidly with intensity, concomitant increases in flow depth with intensity considerably damp sediment delivery. Figure 9 shows that steady state sediment discharge increases approximately linearly with rainfall intensity, despite the nonlinear increase in rain power. This result emphasizes the complex interaction between sediment detachment, flow depths, and sediment delivery in overland flow.

6. Conclusion

[37] The importance of raindrop impact in detaching soil particles that may be transported by overland flow has been often studied and documented. The majority of these investigations have relied on statistical multivariate analyses and have produced a number of different equations relating sediment detachment to parameters such as drop circumference, hillslope angle, and kinetic energy. In this paper, we derive a mathematical expression that reflects the physical interactions that can be observed during rainstorms on rough, steep natural hillslopes. The expression involves the rain power, a quantity that represents the rate of work done by falling raindrops on the soil surface and incorporates rainfall, hillslope, and vegetation characteristics. We

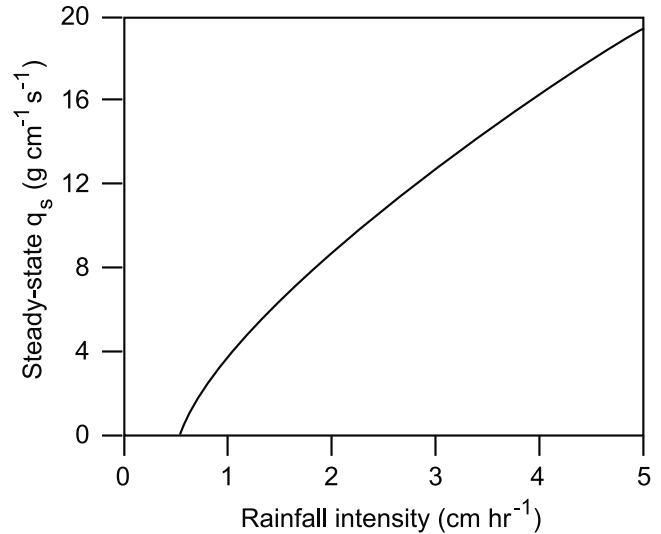


Figure 9. Steady state sediment discharges at different rainfall intensities. Hillslope parameters are the same as in Table 1, except that the vegetation cover is 0.60. Although rain power is nonlinearly dependent on rainfall intensity, sediment discharge increases approximately linearly with rainfall intensity because of the damping effect of greater flow depths.

also develop an attenuation function to account for the decline in detachment rates caused by water on the soil surface. Through a series of rainfall simulation experiments on natural hillslopes, the rain power formulation is tested for its correlation with observed transport rates of sediment that is fine enough to be transported as wash load.

[38] In addition, we examine the process of detachment and its control on soil loss from entire hillslopes. We numerically model sediment detachment rates by rain power and present how detachment rates can be integrated over the length of a hillslope and the duration of a rainstorm, taking into account the effects of gradient, cover density, infiltration capacity, and rainfall intensity. Our results indicate that properly representing across-slope flow depth distributions is critical in understanding and modeling sediment detachment and sediment delivery.

Appendix A: Determination of Manning's n From Recession Limbs

[39] The complex flow paths precluded the possibility of directly determining values for Manning's n by measuring flow depths and velocities. However, it is possible to determine a spatially-averaged flow resistance coefficient through the use of the method of characteristics by analyzing the recession limb. Because the shape of the recession limb (and the rising limb) is a function of both roughness and infiltration capacity, it can be used to estimate Manning's n when the infiltration capacity is known. It would be preferable to determine Manning's n from the rising limb [e.g., Engman, 1986] to include roughness from raindrop impact [Parsons *et al.*, 1994], however, the infiltration capacity changed during the early moments of each rainfall experiment due to the presence of shrink-swell clays. We assume that the contribution to flow resistance made by drop

impact is negligible considering the rough soil surface [Dunne and Dietrich, 1980].

[40] Henderson and Wooding [1964] demonstrated how the method of characteristics could be used to calculate runoff hydrographs from an impermeable surface based on a kinematic wave approximation. Dunne and Dietrich [1980] extended this analysis by allowing infiltration after the end of rainfall. One of the equations derived by Dunne and Dietrich [1980], equation 15 (note: due to a typographical error, the quantity “ α/i ” was omitted from the last term in the original paper), is recast as

$$T = \frac{1}{f} \left\{ h_{ss} - \left[h_{ss}^m - \frac{nf}{\sqrt{s}} (L - x^0) \right]^{1/m} \right\}, \quad (A1)$$

where

- T time for a characteristic beginning at x^0 to reach L ; $T = 0$ at the cessation of rainfall;
- f infiltration capacity;
- h_{ss} steady state depth at x^0 ;
- m value depends on whether the flow is laminar or turbulent (assumed to be 5/3 here);
- s hillslope gradient;
- n Manning's roughness coefficient;
- L length of the hillslope or plot;
- x^0 initial position of the characteristic at $T = 0$.

In the method developed here, a Manning's n is initially estimated, a series of initial positions (x^0, x^T, x^n) are chosen, and steady state depths (h_{ss}) are calculated at each initial position (see Dunne and Dietrich [1980] for details). Because the flow had a distribution of flow depths rather than a uniform thickness, the implied depth scale is the average depth (\bar{h}). The time (T) for a particular characteristic to reach L is calculated with (A1) and the depth of flow (h) for this characteristic when it reaches L is calculated with

$$h = h_{ss} - fT. \quad (A2)$$

The discharge for that characteristic is calculated with (25).

[41] By repeating this procedure with each chosen initial position, the recession limb of a hydrograph can be calculated. An effective Manning's n can then be determined by plotting the calculated recession limb against the recession limb from the field experiments and varying the value of the roughness coefficient until they match. This usually takes 3–4 iterations and is quickly done with a spreadsheet program.

[42] **Acknowledgments.** The rainfall experiments were labor-intensive and would not have been possible without the help of N. Fierer, J. Wikings, C. Zelding, N. Dooling, T. Marden, R. Bryan, K. Kuhn, and M. Singer. Discussions with P. Kinnell and R. Bryan were invaluable. We thank the two anonymous reviewers for their comments that helped us to focus the scope of the paper. We are also grateful for the assistance we received from the staff at the Sedgwick Natural Reserve, including M. Williams and R. Skillin. Supplies and salary for E. Gabet were supported by a U.C. Regents Fellowship, U.C. Water Resources grant UCAL-W-917, and a Sigma Xi grant. Computer modeling supported in part by National Science Foundation grant CDA96-01954 and by Silicon Graphics Inc.

References

Abrahams, A. D., and A. J. Parsons, Resistance to overland flow on desert pavement and its implications for sediment transport modeling, *Water Resour. Res.*, 27(8), 1826–1836, 1991.

- Abrahams, A. D., A. J. Parsons, and S. H. Luk, Distribution of depth of overland flow on desert hillslopes and implications for modeling soil erosion, *J. Hydrol.*, 106, 177–184, 1989.
- Abrahams, A. D., A. J. Parsons, and P. J. Hirsch, Field and laboratory studies of resistance to interrill overland flow on semi-arid hillslopes, southern Arizona, in *Overland Flow: Hydraulics and Erosion Mechanics*, edited by A. J. Parsons and A. D. Abrahams, pp. 1–23, Chapman and Hall, New York, 1992.
- Carter, C. E., J. D. Greer, H. J. Brand, and J. M. Floyd, Raindrop characteristics in south central United States, *Trans. ASAE*, 17, 1033–1037, 1974.
- Dibblee, T. W. J., Geologic map of the Figueroa Mountain Quadrangle, Dibblee Geol. Found., Santa Barbara, Calif., 1993.
- Dunne, T., and B. F. Aubry, Evaluation of Horton's theory of sheetwash and rill erosion on the basis of field experiments, in *Hillslope Processes*, edited by A. D. Abrahams, pp. 31–53, Allen and Unwin, London, 1986.
- Dunne, T., and W. E. Dietrich, Experimental investigation of Horton overland flow on tropical hillslopes, 2, Hydraulic characteristics and hillslope hydrographs, *Z. Geomorphol. Suppl.*, 35, 60–80, 1980.
- Dunne, T., W. Zhang, and B. Aubry, Effects of rainfall, vegetation, and microtopography on infiltration and runoff, *Water Resour. Res.*, 27(9), 2271–2285, 1991.
- Ekern, P. C., Raindrop impact as the force initiating soil erosion, *Soil Sci. Soc. Am. Proc.*, 15, 7–10, 1950.
- Ekern, P. C., Rainfall intensity as a measure of storm erosivity, *Soil Sci. Soc. Am. Proc.*, 18, 212–216, 1954.
- Ellison, W. D., Soil erosion studies, 1, *Agric. Eng.*, 28(4), 145–146, 1947.
- Emmett, W. W., The hydraulics of overland flow on hillslopes, *U.S. Geol. Surv. Prof. Pap.*, 662-A, 1970.
- Engman, E. T., Roughness coefficients for routing surface runoff, *J. Irrig. Drainage Eng. Am. Soc. Civ. Eng.*, 112(1), 39–53, 1986.
- Fierer, N. G., and E. G. Gabet, Transport of carbon and nitrogen by surface runoff from hillslopes in the central coast region of California, *J. Environ. Qual.*, 31, 1207–1213, 2002.
- Foster, G. R., and L. D. Meyer, Mathematical simulation of upland erosion by fundamental erosion mechanics, in *Present and Prospective Technology for Predicting Sediment Yields and Sources, Proceedings of the Sediment Yield Workshop, 1972*, pp. 190–207, U.S. Dep. of Agric., Washington, D. C., 1975.
- Gabet, E. J., Gopher bioturbation: Field evidence for nonlinear hillslope diffusion, *Earth Surf. Processes Landforms*, 25(13), 1419–1428, 2000.
- Gilley, J. E., and S. C. Finkner, Estimating soil detachment caused by raindrop impact, *Trans. ASAE*, 28, 140–146, 1985.
- Gilley, J. E., D. A. Woolhiser, and D. B. McWhorter, Interrill soil erosion, part II, Testing and use of model equations, *Trans. ASAE*, 28, 155–159, 1985.
- Gilley, J. E., D. C. Flanagan, E. R. Kottwitz, and M. A. Weltz, Darcy-Weisbach roughness coefficients for overland flow, in *Overland Flow: Hydraulics and Erosion Mechanics*, edited by A. J. Parsons and A. D. Abrahams, pp. 25–52, Chapman and Hall, New York, 1992.
- Gunn, R., and G. D. Kinzer, The terminal velocity of fall for water droplets in stagnant air, *J. Meteorol.*, 6, 243–248, 1949.
- Hairsine, P. B., and C. W. Rose, Modeling water erosion due to overland flow using physical principles, 1, Sheet flow, *Water Resour. Res.*, 28(1), 237–243, 1992.
- Henderson, F. M., and R. A. Wooding, Overland flow and groundwater flow from a steady rainfall of finite duration, *J. Geophys. Res.*, 69, 1531–1540, 1964.
- Hudson, N. W., Erosion control research, *Rhodesia Agric. J.*, 54(4), 297–323, 1957.
- Iverson, R. M., Processes of accelerated pluvial erosion on desert hillslopes modified by vehicular traffic, *Earth Surf. Processes Landforms*, 5, 369–388, 1980.
- Jayawardena, A. W., and R. B. Rezaur, Drop size distributions and kinetic energy load of rainstorms in Hong Kong, *Hydrol. Processes*, 14, 1069–1082, 2000.
- Kinnell, P. I. A., The influence of flow discharge on sediment concentrations in raindrop induced flow transport, *Aust. J. Soil Sci.*, 26, 575–582, 1988.
- Kinnell, P. I. A., The mechanics of raindrop-induced flow transport, *Aust. J. Soil Sci.*, 28, 497–516, 1990.
- Kinnell, P. I. A., The effect of flow depth on sediment transport induced by raindrops impacting shallow flows, *Am. Soc. Agric. Eng.*, 34(1), 161–168, 1991.
- Kinnell, P. I. A., Sediment concentrations resulting from flow depth/drop size interactions in shallow overland flow, *Trans. ASAE*, 36(4), 1099–1103, 1993a.

- Kinnell, P. I. A., Sediment transport by shallow flows impacted by pulsed artificial rainfall, *Aust. J. Soil Sci.*, 31, 199–207, 1993b.
- Kinnell, P. I. A., and J. T. Wood, Isolating erosivity and erodibility components in erosion by rain-impacted flow, *Trans. ASAE*, 35(1), 201–205, 1992.
- Kneale, W. R., Field measurements of rainfall drop size distribution, and the relationships between rainfall parameters and soil movement by rainsplash, *Earth Surf. Processes Landforms*, 7, 499–502, 1982.
- Krumbein, W. C., and F. A. Graybill, *An Introduction to Statistical Models in Geology*, McGraw-Hill, New York, 1965.
- Laws, J. O., Measurements of the fall velocity of water-drops and raindrops, *Eos Trans. AGU*, 21, 709–721, 1941.
- Laws, J. O., and D. A. Parsons, The relation of raindrop size to intensity, *Eos Trans. AGU*, 24, 452–459, 1943.
- Lima, J. L. M. P. D., Model KININF for overland flow on pervious surfaces, in *Overland Flow: Hydraulics and Erosion Mechanics*, edited by A. J. Parsons and A. D. Abrahams, pp. 69–88, Chapman and Hall, New York, 1993.
- McCarthy, C. J., Sediment transport by rainsplash, Ph.D. thesis, 215 pp., Univ. of Wash., Seattle, 1980.
- McCool, D. K., L. C. Brown, G. R. Foster, C. K. Mutchler, and L. D. Meyer, Revised slope steepness factor for the Universal Soil Loss Equation, *Trans. ASAE*, 30(5), 1387–1396, 1987.
- Meyer, L. D., How rain intensity affects interrill erosion, *Trans. ASAE*, 24, 1472–1475, 1981.
- Morgan, R. P. C., Field studies of sediment transport by overland flow, *Earth Surf. Processes*, 5(4), 307–316, 1980.
- Moss, A. J., and P. Green, Movement of solids in air and water by raindrop impact: Effects of drop-size and water-depth variations, *Aust. J. Soil Res.*, 21, 257–269, 1983.
- Mutchler, C. K., and K. C. McGregor, Erosion from low slopes, *Water Resour. Res.*, 19(5), 1323–1326, 1983.
- Nearing, M. A., G. R. Foster, L. J. Lane, and S. C. Finkner, A process-based soil erosion model for USDA-Water Erosion Prediction Project, *Trans. ASAE*, 32, 1587–1593, 1989.
- Palmer, R. S., Waterdrop impact forces, *Trans. ASAE*, 8(1), 169–70, 72, 1965.
- Palmer, V. J., Retardance coefficients for low flow in channels lined with vegetation, *Trans. ASAE*, 27(2), 187–197, 1946.
- Parsons, A. J., and A. D. Abrahams, Field investigations of sediment removal in interrill overland flow, in *Overland Flow: Hydraulics and Erosion Mechanics*, edited by A. J. Parsons and A. D. Abrahams, pp. 307–334, Chapman and Hall, New York, 1992.
- Parsons, A. J., and A. M. Gadian, Uncertainty in modelling the detachment of soil by rainfall, *Earth Surf. Processes Landforms*, 25, 723–728, 2000.
- Parsons, A. J., A. D. Abrahams, and J. Wainwright, On determining resistance to interrill overland flow, *Water Resour. Res.*, 30(12), 3515–3521, 1994.
- Reid, L. M., and T. Dunne, *Rapid Evaluation of Sediment Budgets*, Catena, Reiskirchen, Germany, 1996.
- Roels, J. M., Flow resistance in concentrated overland flow on rough slope surfaces, *Earth Surf. Processes Landforms*, 9, 541–551, 1984.
- Rouhipour, H., C. W. Rose, B. Yu, and H. Ghadir, Roughness coefficients and velocity estimation in well-inundated sheet and rilled overland flow without strongly eroding bed forms, *Earth Surf. Processes Landforms*, 24, 233–245, 1999.
- Salles, C., J. Poesen, and L. Borselli, Measurement of simulated drop size distribution with an optical spectro pluviometer: Sample size considerations, *Earth Surf. Processes Landforms*, 24, 545–556, 1999.
- Salles, C., J. Poesen, and G. Govers, Statistical and physical analysis of soil detachment by raindrop impact: Rain erosivity indices and threshold energy, *Water Resour. Res.*, 36(9), 2721–2729, 2000.
- Schmidt, J., Modelling long-term soil loss and landform change, in *Overland Flow: Hydraulics and Erosion Mechanics*, edited by A. J. Parsons and A. D. Abrahams, pp. 409–433, Chapman and Hall, New York, 1993.
- Schultz, J. P., A. R. Jarret, and J. R. Hoover, Detachment and splash of a cohesive soil by rainfall, *Trans. ASAE*, 28, 1878–1884, 1985.
- Shipman, G. E., Soil survey of northern Santa Barbara area, California, Soil Conserv. Serv., Washington, D. C., 1972.
- Smith, D. D., and W. H. Wischmeier, Rainfall erosion, *Adv. Agron.*, 14, 109–148, 1962.
- Wischmeier, W. H., A rainfall erosion index for a universal soil-loss equation, *Soil Sci. Soc. Am. Proc.*, 23(3), 246–249, 1959.
- Woolhiser, D. A., Simulation of unsteady overland flow, in *Unsteady Flow in Open Channels*, edited by K. Mahmood and V. M. Yevjevich, pp. 485–508, Water Resour. Publ., Highlands Ranch, 1975.
- Woolhiser, D. A., and J. A. Liggett, One-dimensional flow over a plane: The rising hydrograph, *Water Resour. Res.*, 3(3), 753–771, 1967.
- Young, R. A., and J. L. Wiersma, The role of rainfall impact in soil detachment and transport, *Water Resour. Res.*, 9(6), 1629–1636, 1973.
- Zhang, X. C., M. A. Nearing, W. P. Miller, L. D. Norton, and L. T. West, Modeling interrill sediment delivery, *Soil Sci. Soc. Am. J.*, 62, 438–444, 1998.

T. Dunne, Donald Bren School of Environmental Science and Management and Department of Geological Sciences, University of California, Santa Barbara, Santa Barbara, CA 93106, USA.

E. J. Gabet, Department of Geological Sciences, University of California, Santa Barbara, CA 93106, USA. (egabet@bren.ucsb.edu)